Organic & Biomolecular Chemistry

ROYAL SOCIETY OF CHEMISTRY

COMMUNICATION

View Article Online
View Journal | View Issue

Cite this: *Org. Biomol. Chem.*, 2023, **21**, 3079

Received 23rd February 2023,
Accepted 14th March 2023

DOI: 10.1039/d3ob00302g

rsc.li/obc

Aminophthalimide as a mimetic of purines and a fluorescent RNA base surrogate for RNA imaging†

Fabian Lang, Franziska Rönicke and Hans-Achim Wagenknecht *

Aminophthalimide and *N*,*N*-dimethylaminophthalimide are used as fluorescent mimetics of purines due to their similar size and their possibility for hydrogen bonding. Their C-nucleotides were synthetically incorporated into RNA by means of phosphoramidite chemistry, behave as nonspecific fluorescent base analogs with flexible hydrogen bonding capabilities, and show solvatochromic fluorescence that is suitable for RNA imaging in live cells.

Imaging of RNA in living cells becomes increasingly important to visualize and study the diverse biological processes of RNA in real time. Fluorescent base analogs have the advantage that they can be placed precisely in any desired RNA base sequence.[1–6] The challenge is to design fluorescent RNA base surrogates that do not alter the structure and biological function of RNA, or at least not to a significant extent. Base surrogates follow this principle (Fig. 1). Probably the most extensively used is 2-aminopurine (2-Ap),[7–9] initially presented by Reich and Stryer in 1969.[10] For instance, it has been successfully applied to study RNA folding.[11] The optical key parameters of 2-aminopurine, however, are rather poor: excitation in the UV-B range (305 nm), a low extinction coefficient that interferes with the RNA absorbance, and fluorescence in the UV-A range (370 nm) that is quenched in double-stranded DNA by charge transfer processes. Pyrrolocytosine, introduced in 2004 by Berry *et al.*,[12] is not much different and shows also a low fluorescence quantum yield. To overcome these limitations, Damha *et al.* presented a phenylpyrrolocytosine for monitoring the cellular trafficking of siRNA.[13] Using alternative basic structures, Wilhelmsson *et al.* designed 1,3-diaza-2-oxophenoxazines (tC^O) as stealth fluorescent labels for imaging of mRNA delivery to cells.[14] Tor *et al.* established a whole set of fluorescent and isomorphic thienonucleoside surrogates, for instance the G analog ^{th}G, as an emissive "RNA alphabet".[15,16] They all, in common, bind specifically to one of the natural RNA components as complementary counterbases. This restricts their usage to specific sites given by the sequence of the RNA probe. A universal fluorescent base analog without specific base pairing is still elusive. We established 4-aminophthalimide as a mimetic and solvatochromic surrogate of tryptophane in transmembrane peptides[17] and as a base surrogate with the size of purines in DNA.[18,19] The NMR structures of this modified DNA revealed that only two out of three possible H bonds at the imide side are actually formed, even with 2,4-diaminopyrimidine as the fully complementary nucleoside. A "sliding" of the hydrogen-bonding interface was observed due to the geometry of the H-bonding interface which gives

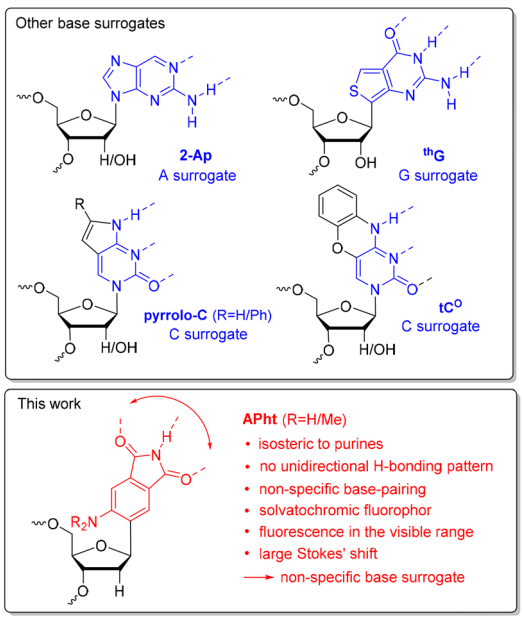

Fig. 1 2-Aminopurine (2-Ap), thieno-G (^{th}G), pyrrolo-C and 1,3-diaza-2-oxophenoxazine (tC^O) as specific fluorescent base analogs for RNA in comparison to the C-nucleosides of aminophthalimide as a non-specific base surrogate.

Institute of Organic Chemistry, Karlsruhe Institute of Technology (KIT), Fritz-Haber-Weg 6, 76131 Karlsruhe, Germany. E-mail: Wagenknecht@kit.edu

† Electronic supplementary information (ESI) available: Methods, MS data, and optical spectroscopy. See DOI: https://doi.org/10.1039/d3ob00302g

the chromophore a flexible H-bonding capability. Herein, we characterize 4-aminophthalimide as a fluorescent base surrogate in RNA and show evidence that it can be applied for RNA imaging in cells.

We used the 2′-deoxynucleosides of aminophthalimide **1** and of *N*,*N*-dimethylaminophthalimide **2** as building blocks for the RNA synthesis although they are lacking the 2′-hydroxy group, but they have the advantage that we can rely on our established synthesis protocols.[20] Both nucleosides were incorporated into the representative 13mer oligonucleotide sequences **RNA1** and **RNA2** (Fig. 2) using automated solid-phase syntheses, ultra-mild deprotectable RNA building blocks,[21] and a special procedure for RNA cleavage from solid phase and deprotection. The sequences of **RNAA–RNAU** are complementary and place each of the natural RNA units A, C, G and U opposite to the modification site in **RNA1** and **RNA2** to check how much the fluorescence depends on these counterbases. **RNAS** contains an abasic site analog (spacer, Spa) at this position to allow the best possible intercalation of the aminophthalimide chromophores. **RNAD** contains the 2,4-diaminopyridimidine nucleoside (Dap) as the designed counterbase to the aminophthalimide,[19] because it provides three possibilities for hydrogen bonding in the right order to bind to the imide functionality of the aminophthalimides. All synthetic RNA strands were purified by semi-preparative HPLC, quantified by UV/vis absorbance spectroscopy, and identified by MALDI-TOF mass spectrometry (Fig. S1–S3†).

Melting temperature analysis shows the highest value of 64.5 °C for the duplex **RNA1–RNAD**, indicating that the designed complementary base pair between the aminophthalimide and diaminopyrimidine moieties stabilizes this duplex by the best possible intercalation of the aminophthalimide chromophore. The other RNA duplexes have quite similar melting temperatures in the range of 59–63 °C, indicating that there is no significant base pairing preference of the aminophthalimide nucleoside. The duplex **RNA1–RNAS** with the abasic site spacer, however, shows the lowest melting temperature of 58.7 °C because there is no H-bonded base pairing possible for 4-aminophthalimide. This is an interesting result because it indicates that 4-aminophthalimide needs H-bonding with the counterbase to stack and thereby stabilize the duplex. There is a slight preference for pyrimidine counterbases according to the higher melting temperatures obtained for **RNA1–RNAC**, **RNA1–RNAU**, and **RNA1–RNAD**. There is no difference in the melting temperatures between **RNA1–RNAC** and **RNA1–RNAD** which indicates, similar to our previous results,[18,20] that the third H-bond is not closed. The duplex **RNA1–RNAC** shows, however, an initial hypochromism between 10 °C and 45 °C (Fig. S8†), indicating a better stacking with the flanking nucleobases upon heating in this temperature range, which is contrary to what is typically seen with unmodified RNA double-strands and also observed for the other duplexes of **RNA1**. This behavior was already explained for the **APht1** modification in DNA by theoretical calculations and NMR spectroscopy:[18] at very low temperatures, the chromophore of **APht1** is bound by only one H-bond to the counterbase and thus located partially outside the DNA helix. This allows only stacking with the bases in the 3′-direction. With increasing temperature, the second H-bond is formed which enforces complete stacking of the chromophore in both directions of the helix. Because the cell imaging experiments are typically performed at such elevated temperatures (37 °C), this structural behavior makes the duplex **RNA1–RNAC** best suitable for cell experiments. The melting temperatures of the duplexes of **RNA2** lie in the range of 56–59 °C and do not show a pattern comparable to the double-strands of **RNA1**. Obviously, the steric hindrance of the dimethylamino group interferes with the stability of the RNA duplexes because the melting temperatures of the duplexes with **RNA2** are all a few degrees lower than those obtained with the duplexes of **RNA1**. Because there seems to be no obviously preferred H-bonding pattern in the duplexes with **RNA1** and **RNA2**, the aminophthalimide in **RNA1** and the *N*,*N*-dimethylaminophthalimide in **RNA2** can be considered as non-specific base surrogates with flexible H-bonding capabilities (Table 1).

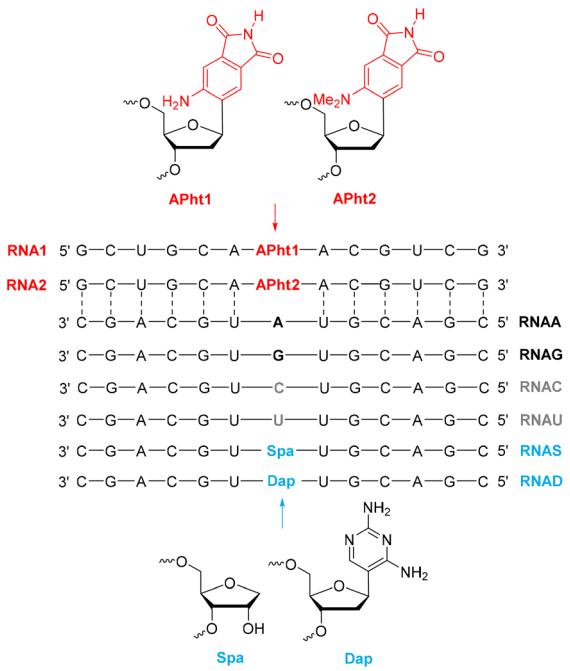

Fig. 2 Sequences of **RNA1** and **RNA2** modified with the aminophthalimide nucleotides **APht1** and **APht2**, respectively, and complementary counterstrands **RNAA–RNAU** (unmodified), **RNAS** and **RNAD** (modified).

Table 1 Melting temperatures (T_m) of the duplexes of **RNA1** and **RNA2** with **RNAX** (X = A, G, C, U, S, D); 2.5 μM RNA, 10 mM NaP_i-buffer, 250 mM NaCl, pH 7, 20 °C. For complete melting profiles, see Fig. S6 and S17†

T_m [°C]	RNAA	RNAG	RNAC	RNAU	RNAS	RNAD
RNA1	60.8	59.0	62.7	62.1	58.7	62.8
RNA2	58.2	57.2	56.2	58.9	55.8	56.7

The artificial nucleobases **APht1** and **Apht2** add very weak absorption bands in the UV-A range of 350–450 nm to the UV-B absorption range of the nucleic acid (Fig. S4 and S5†) which can be used to selectively excite these fluorophores. The aminophthalimide fluorescence maxima lie in the range of 510 nm to 529 nm (Fig. 3). These solvatofluorescence properties reflect the extent of stacking of the aminophthalimide chromophore within the RNA duplex. The strongest shift to smaller wavelengths is observed for **RNA1–RNAC** (510 nm) indicating a well-stacked chromophore, compared to the single-stranded **RNA1** (527 nm), whereas **RNA1–RNAU** (529 nm) does not show any significant shift. In the latter duplex, obviously the imide functions of the aminophthalimide and uridine interfere with each other and prevent the stacking of the chromophore to a significant extent. The duplex **RNA1–RNAC** shows the highest fluorescence intensity associated with a significant hypsochromic shift, which indicates stronger stacking interactions of the chromophore in this duplex based on the solvatochromism of the **Apht1** fluorescence.[18–20] The other duplexes of **RNA1** follow the order **RNAS** > **RNAD** > **RNAA** ~ **RNAG** ~ **RNAU**. Neither the fluorescence maxima nor the fluorescence intensities of the duplexes with **RNA1** and **RNA2** do track with the differences in the melting temperatures. But it is important to note that all duplexes show a significantly higher fluorescence intensity than the single-stranded **RNA1**. This is the reason why we consider aminophthalimide as a non-specific fluorescent base surrogate for RNA; we see an enhanced fluorescence intensity for all the duplexes. It was assumed that the fluorescence quantum yields of the **APht1** nucleoside in RNA are similar to those obtained in DNA (15–24%).[20] In comparison, the fluorescence intensities of single-stranded **RNA2** and its corresponding duplexes are all nearly one magnitude of order smaller and red-shifted. These low fluorescence intensities do not allow any detailed discussions and are not suitable for fluorescence RNA imaging. Obviously, the dimethylamino group reduces the fluorescence intensity by non-radiative decays *via* TICT states.[22] Only the duplex **RNA2–RNAA** shows a higher fluorescence intensity with a bathochromically shifted maximum (552 nm) compared to the single-stranded **RNA2** (538 nm) Overall, only the non-methylated 4-aminophthalimide as a fluorophor in **RNA1** shows fluorescence intensities sufficient for RNA imaging, most pronounced in the case of **RNA1–RNAC**.

To elucidate the biocompatibility and imaging properties of the **RNA1–RNAC** sample, we transfected HeLa cells for 24 hours with Lipofectamine®2000 and subsequently analyzed the transfected cells by confocal fluorescence microscopy. Therefore, we used 125 ng of the **RNA1–RNAC** construct, allowed the RNA to form lipoplexes with the corresponding Lipofectamine solution and finally mixed it with 4×10^4 cells and seeded them into an 8-well μ-slide (IBIDI, Ibitreat). After 24 hours, the cells were washed with PBS and subjected to microscopy. **RNA1–RNAC** was excited with a 405 nm laser and emission was measured at 500–580 nm, complemented with a brightfield image. As a negative control, we used aminophthalimide as an isolated chromophore, to make sure that our signal definitely derives from the intact **RNA1–RNAC** probe. With this approach, we could demonstrate that the pattern of the actual probe is clearly different from the negative control, which only shows an evenly distributed, slight background fluorescence (Fig. 4). However, the cells transfected with the **RNA1–RNAC** construct bring out a distinct fluorescent pattern primarily inside vesicular structures, demonstrating the strong accumulation of **RNA1–RNAC** probably in endosomal vesicles. The strong and clear fluorescence signal in these experiments thus allows the conclusion that the C-nucleotides of aminophthalimide, as used in the experiments integrated in a double stranded construct with **RNA1**, are stable enough to remain intact during the transfection and microscopy procedure.

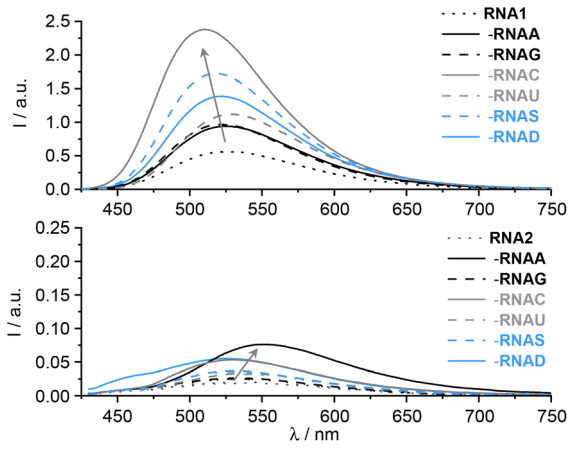

Fig. 3 Fluorescence of the single-stranded **RNA1** (top), **RNA2** (bottom), and the corresponding duplexes with **RNAA–RNAD**; 2.5 μM RNA, 10 mM Na–P_i buffer, 250 mM NaCl, pH 7, 20 °C, λ_{exc} = 385 nm (**RNA1**) 410 nm (**RNA2**), slits 3/3 nm (**RNA1**), 9/9 nm (**RNA2**).

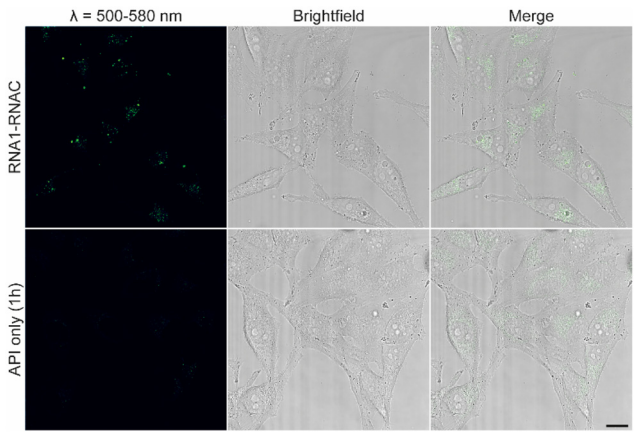

Fig. 4 HeLa cells after 24 h transfection with **RNA1–RNAC** (125 ng), imaged by confocal fluorescence microscopy with a 405 nm laser line and an emission channel at 500–580 nm, complemented with a brightfield channel. As a negative control, HeLa cells were treated only with aminophthalimide for 1 h. Scale bar: 30 μm.

Conclusions

The C-nucleotides of aminophthalimide and *N*,*N*-dimethylaminophthalimide were synthesized and incorporated as purine surrogates into single- and double-stranded RNA. They behave as non-specific fluorescent base analogs for single- and double-stranded RNA because there is no canonical base-pairing detectable, neither by melting temperatures nor by fluorescence. The imide functionality in the five-membered ring of the aminophthalimide provides a hydrogen-bonding interface that needs H-bonding with the counterbase, but not in a specific and directed way. This has the advantage that the aminophthalimide nucleotide may replace any of the natural nucleotides in any given RNA sequence at a desired position. In all cases, the aminophthalimide shows fluorescence in the visible range with a large Stokes shift, which is suitable for RNA imaging in live cells. The phthalimide unit is stable enough to remain intact during the transfection and microscopy procedure. This means that the implementation of this fluorescent base surrogate is clearly applicable for future biological studies in living cells.

Author contributions

FL synthesized the nucleosides and the RNA single strands and performed all optical–spectroscopic experiments. FR performed the cell experiments. HAW supervised the research and wrote major parts of the manuscript.

Conflicts of interest

There are no conflicts to declare.

Acknowledgements

Financial suport by the Deutsche Forschungsgemeinschaft (grant Wa 1386/17-2) and KIT is gratefully aknowledged.

References

1 M. E. Hawkins, *Cell Biochem. Biophys.*, 2001, **34**, 257–280.
2 Y. N. Teo and E. T. Kool, *Chem. Rev.*, 2012, **112**, 4221–4245.
3 R. W. Sinkeldam, N. J. Greco and Y. Tor, *Chem. Rev.*, 2010, **110**, 2579–2619.
4 L. M. Wilhelmsson, *Q. Rev. Biophys.*, 2010, **43**, 159–183.
5 A. A. Tanpure, M. G. Pawar and S. G. Srivatsan, *Isr. J. Chem.*, 2013, **53**, 366–378.
6 Y. Saito and R. H. E. Hudson, *J. Photochem. Photobiol., A*, 2018, **36**, 48–73.
7 M. J. Rist and J. P. Marino, *Curr. Org. Chem.*, 2002, **6**, 775–793.
8 M. Kawai, M. J. Lee, K. O. Evans and T. M. Nordlund, *J. Fluoresc.*, 2001, **11**, 23–32.
9 A. Dallmann, L. Dehnel, T. Peters, C. Mügge, C. Griesinger, J. Tuma and N. P. Ernsting, *Angew. Chem., Int. Ed.*, 2010, **49**, 5989–5992.
10 D. C. Ward, E. Reich and L. Stryer, *J. Biol. Chem.*, 1969, **244**, 1228–1237.
11 M. F. Soulière, A. Haller, R. Rieder and R. Micura, *J. Am. Chem. Soc.*, 2011, **133**, 16161–16167.
12 D. A. Berry, K.-Y. Jung, D. S. Wise, A. D. Sercel, W. H. Pearson, H. Mackie, J. B. Randolph and R. L. Somers, *Tetrahedron Lett.*, 2004, **45**, 2457–2461.
13 A. S. Wahba, F. Azizi, G. F. Deleavey, C. Brown, F. Robert, M. Carrier, A. Kalota, A. M. Gewirtz, J. Pelletier, R. H. E. Hudson and M. J. Damha, *ACS Chem. Biol.*, 2011, **6**, 912–919.
14 T. Baladi, J. R. Nilsson, A. Gallud, E. Celauro, C. Gasse, F. Levi-Acobas, I. Sarac, M. R. Hollenstein, A. Dahlén, E. K. Esbjörner and L. M. Wilhelmsson, *J. Am. Chem. Soc.*, 2021, **143**, 5413–5424.
15 D. Shin, P. Lönn, S. F. Dowdy and Y. Tor, *Chem. Commun.*, 2015, **51**, 1662–1665.
16 I. Paul, T. Ludford, S. Yang, M. S. Bucardo and Y. Tor, *Chem. – Eur. J.*, 2022, **28**, e2021004472.
17 S. Wörner, F. Rönicke, A. S. Ulrich and H.-A. Wagenknecht, *ChemBioChem*, 2020, **21**, 618–622.
18 L. Dehmel, F. Berndt, M. Weinberger, M. Sajadi, I. Ioffe, H.-A. Wagenknecht and N. P. Ernsting, *Phys. Chem. Chem. Phys.*, 2016, **18**, 6813–6820.
19 M. Weinberger, F. Berndt, R. Mahrwald, N. P. Ernsting and H.-A. Wagenknecht, *J. Org. Chem.*, 2013, **78**, 2589–2599.
20 M. Merkel, L. Dehmel, N. P. Ernsting and H.-A. Wagenknecht, *Angew. Chem., Int. Ed.*, 2017, **56**, 384–388.
21 J. C. Schulhof, D. Molko and R. Teoule, *Nucleic Acids Res.*, 1987, **15**, 397–416.
22 T. Soujanya, R. W. Fessenden and A. Samanta, *J. Phys. Chem.*, 1996, **100**, 3507–3512.